JACS
JOURNAL OF THE AMERICAN CHEMICAL SOCIETY

Article

pubs.acs.org/JACS

Dynamical Disorder in the DNA Hydration Shell

Elise Duboué-Dijon,[†,‡,∥] Aoife C. Fogarty,[†,‡,∥,⊥] James T. Hynes,*[,†,‡,§] and Damien Laage*[,†,‡]

[†]École Normale Supérieure, PSL Research University, UPMC Univ Paris 06, CNRS, Département de Chimie, PASTEUR, 24 rue Lhomond, 75005 Paris, France

[‡]Sorbonne Universités, UPMC Univ Paris 06, ENS, CNRS, PASTEUR, 75005 Paris, France

[§]Department of Chemistry and Biochemistry, University of Colorado, Boulder, Colorado 80309-0215, United States

Supporting Information

ABSTRACT: The reorientation and hydrogen-bond dynamics of water molecules within the hydration shell of a B-DNA dodecamer, which are of interest for many of its biochemical functions, are investigated via molecular dynamics simulations and an analytic jump model, which provide valuable new molecular level insights into these dynamics. Different sources of heterogeneity in the hydration shell dynamics are determined. First, a pronounced spatial heterogeneity is found at the DNA interface and explained via the jump model by the diversity in local DNA interfacial topographies and DNA−water H-bond interactions. While most of the hydration shell is moderately retarded with respect to the bulk, some water molecules confined in the narrow minor groove exhibit very slow dynamics. An additional source of heterogeneity is found to be caused by the DNA conformational fluctuations, which modulate the water dynamics. The groove widening aids the approach of, and the jump to, a new water H-bond partner. This temporal heterogeneity is especially strong in the minor groove, where groove width fluctuations occur on the same time scale as the water H-bond rearrangements, leading to a strong dynamical disorder. The usual simplifying assumption that hydration shell dynamics is much faster than DNA dynamics is thus not valid; our results show that biomolecular conformational fluctuations are essential to facilitate the water motions and accelerate the hydration dynamics in confined groove sites.

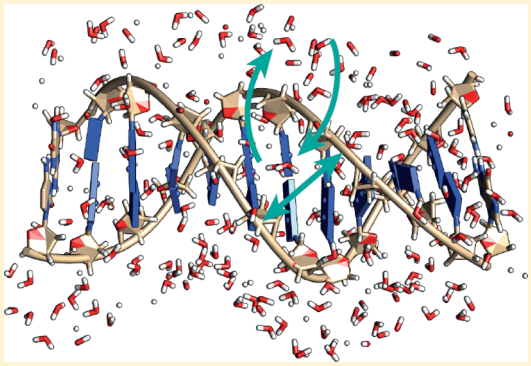

INTRODUCTION

The layer of water molecules surrounding a double-stranded DNA plays an essential role in both preserving the DNA structure and ensuring its proper biochemical function. DNA's conformation depends sensitively on the hydration level: upon dehydration, the iconic double-helical B-form is replaced by other conformations.[1] The hydration layer further protects the delicate double-helix structure from an excess of heat, and provides efficient, rapid dissipation of energy resulting from e.g. a UV photon absorption before it breaks the hydrogen-bonds (H-bonds) between DNA bases.[2] The hydration layer is moreover involved both in processing the genetic information encoded in DNA, e.g., in the recognition and binding of restriction enzymes, and in DNA−ligand interactions,[3,4] including protein binding[5] and perhaps most notably the intercalation of anticancer drugs between DNA base pairs.[6,7] Such processes require a significant displacement and rearrangement of water molecules surrounding the DNA.

The properties of DNA's hydration shell have thus been extensively studied,[1,3,8−36] with special attention devoted to its dynamics. Despite considerable progress, important aspects of the molecular character of these dynamics remain unclear; further, consensus has not yet been achieved on the molecular origin—or sometimes even the existence—of some dynamical features. A key question in the latter category is the potential presence of some very slow water molecules in the vicinity of DNA. Both issues are relevant for the processes mentioned above. For example, these slower dynamics could induce an important friction on ligand approach and affect the binding kinetics,[37] or impede motion over the transition state in drug interaction.[6]

A broad range of techniques has been employed to probe nucleic acid hydration dynamics, including time-dependent Stokes shift (TDSS) experiments,[9,12,13] NMR,[8,11,14−18] and ultrafast infrared[19,20] spectroscopies, dielectric relaxation,[21] neutron scattering,[38,39] and molecular dynamics simulations.[10,22−32,40]

Magnetic relaxation dispersion experiments[8] on a DNA dodecamer duplex led to the conclusion that water dynamics within the DNA hydration layer experience on average a moderate 6-fold slowdown factor with respect to the bulk at ambient temperature (without revealing the source of this slowdown); the exception is a set of five water molecules with much longer estimated residence times (∼200 ps). These very slow water molecules were tentatively located in the DNA minor groove, where an X-ray study had revealed a string of ordered water molecules, termed the "spine of hydration".[34]

Received: March 14, 2016
Published: May 30, 2016

DOI: 10.1021/jacs.6b02715
J. Am. Chem. Soc. 2016, 138, 7610−7620

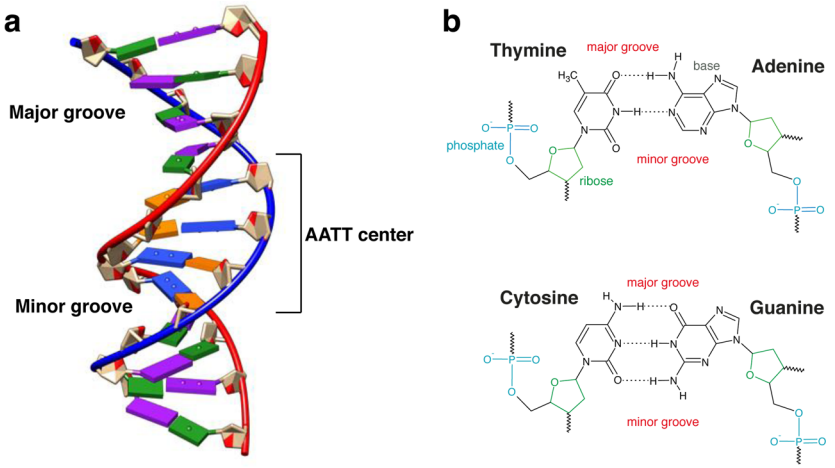

Figure 1. (a) Schematic representation of the Dickerson-Drew DNA dodecamer, with the different nucleobases highlighted in color (adenine in blue, thymine in orange, cytosine in green, and guanine in purple). (b) Pairs of nucleotides showing the nucleobases (black), the deoxyribose sugars (green), and the phosphate groups (cyan).

TDSS experiments[9,12,13] offered the first time-resolved picture of DNA hydration dynamics, by probing the solvation dynamics of a synthetic DNA base or a groove-bound chromophore. Beyond more rapid dynamics, a "slow" component was measured in different TDSS relaxation experiments, but with a very large span of measured time scales, ranging from 20 ps[9,12] (i.e., 15 times slower than in bulk water) to tens of ns.[13] The moderately slow 20 ps component was assigned to strongly DNA-bound ordered water molecules.[9] But there is not agreement on this point (see, e.g., refs 30 and 41), since subsequent simulations concluded this 20 ps time scale to instead arise from slow DNA conformational motions.[30]

Molecular dynamics simulations suggested that the water H-bond dynamics and residence time within the DNA hydration shell span a broad range of time scales, with a slow component ranging between a few tens and a few hundreds of ps (see, e.g., refs 10 and 32), but its origin has remained largely elusive.[32] These results show that there is no agreement on the time scale and origin of any slow dynamics, as we noted initially.

In view of this wide span of divergent views and results, the goal of the present study is to provide a comprehensive analysis of water reorientation and H-bond dynamics in the DNA hydration shell. We deal with the interpretation of the basic molecular character of the dynamics on all time scales, but we place a particular focus on the issue of the presence of especially slow water dynamics and identify the molecular origin of these dynamics.

The paradigm system selected for our investigation is the Dickerson-Drew DNA dodecamer duplex d(CGCGAATTC-GCG)$_2$ (Figure 1a) whose hydration layer has already been extensively studied.[8,11,14,22,24,34] Using classical molecular dynamics (MD) simulations, we first systematically determine the water reorientation dynamics within the hydration layer, in order to reveal how different DNA sites induce dramatically different dynamical perturbations in the shell. The molecular level aspects of the relevant DNA features responsible for the different time scales of the hydration dynamics slowdown compared to the bulk are identified through the molecular jump model developed by two of us;[42] this allows us to distinguish, e.g., the respective roles of confinement, of excluded volume effects and of the strengths of the H-bonds between water and each DNA site. The interpretative power of the jump model—which connects the reorientation to the exchange of a water molecule's H-bond partners—has dictated our choice of the water reorientation dynamics for examination rather than, e.g., time-dependent solvation dynamics. The reorientation dynamics are also directly accessible via NMR relaxation experiments, as noted above. We then focus on the sites where water dynamics are the slowest, which we find located in the center of the DNA minor groove. We show that the slow water dynamics in these sites are strongly connected to DNA conformational motions. The similar time scales of the DNA fluctuations and of the water H-bond exchanges lead to a pronounced dynamical disorder,[43] whose molecular origin is finally elucidated.

RESULTS AND DISCUSSION

Spatial Heterogeneity. We first analyze the MD trajectory of the DNA dodecamer in aqueous solution and probe the dynamics of each water molecule within the DNA hydration shell through the molecular reorientation time-correlation function (TCF) measured in ultrafast infrared experiments,[19]

$$C_{\mathrm{reor}}(t) = \langle P_2[\mathbf{u}(0)\cdot\mathbf{u}(t)]\rangle \quad (1)$$

and its associated reorientation time accessible by NMR,[8]

$$\tau_{\mathrm{reor}} = \int_0^\infty C_{\mathrm{reor}}(t)\mathrm{d}t \quad (2)$$

Here $\mathbf{u}(t)$ is the vector direction of the water OH bond at time t and P_2 is the second-order Legendre polynomial. This reorientation focus also has the advantage of allowing a detailed molecular analysis via the molecular jump model,[42] provided in this work.

Figure 2 presents the reorientation TCF (eq 1) averaged over all water molecules initially lying in the dodecamer's first hydration shell (see Methods). The semilogarithmic scale underlines the important feature that the decay markedly deviates from a single-exponential relaxation; this shows that a broad distribution of time scales governs the hydration shell dynamics, including slow components of multiple tens of ps, and this implies the presence of one or more types of heterogeneity.

In order to identify the microscopic origins of this heterogeneity, we consider each DNA exposed site individually

DOI: 10.1021/jacs.6b02715
J. Am. Chem. Soc. 2016, 138, 7610−7620

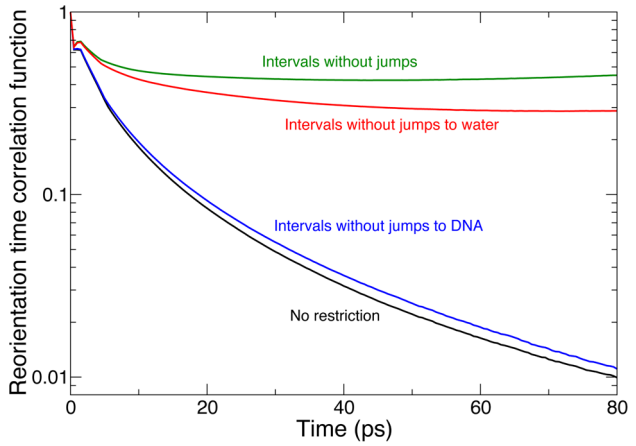

Figure 2. Average reorientation TCF $C_{reor}(t)$ (eq 1) for a water molecule initially in the DNA hydration shell (black), and during intervals when it does not jump to a new water (red) or DNA (blue) acceptor, or to any new H-bond acceptor (green).

and calculate τ_{reor} (eq 2) for the subset of shell water molecules closest to this site (see Methods). The resulting map of τ_{reor} onto the dodecamer surface (Figure 3a) provides a global description of DNA hydration dynamics, with unprecedented molecular level resolution of its *spatial heterogeneity*, i.e., variations over the sites. Most of the hydration shell is found to be only moderately retarded with respect to the bulk (τ_{reor}^{bulk} = 1.7 ps), e.g., next to the ribose groups (see Figure 1). The slowest hydration dynamics are found in the narrowest part of the minor groove, next to the adenine·thymine (A·T) base pairs in the AATT center (see Figure 1). Sites in the major groove and along the phosphate backbone (see Figure 1) induce a more limited dynamical perturbation. (The magnitude and the origin of the retardation induced at each DNA site are further discussed below.)

The average slowdown experienced by shell water molecules relative to the bulk is more easily quantified via the τ_{reor} distribution in Figure 3b. Our calculations yield an average retardation factor of $\langle\rho\rangle_{shell} = \langle\tau_{reor}\rangle^{shell}/\tau_{reor}^{bulk} \simeq 4$ (Figure 3c), in good agreement with the 5−6 value determined by NMR outside the minor groove.[8] This moderate average slowdown results from the combination of several influences: the weak perturbation ($\rho < 4.5$) experienced by a large fraction of the shell and the more pronounced retardation (up to $\rho \simeq 50$) affecting the rest of the shell (Figure 3b,c). We note that this distribution is strikingly similar to distributions calculated[44,45] for globular proteins; these also exhibit a large peak at moderate slowdown values and a long tail corresponding to more strongly retarded water molecules.

Turning to a more molecular perspective, the distribution of reorientation times can be fruitfully decomposed by type of DNA site, distinguishing between hydrophobic, H-bond donor and H-bond acceptor sites (Figure 3b,c). These groups induce different kinds of perturbation on water dynamics and this categorization has already been shown to provide considerable insight into the biomolecular context in prior work on protein hydration shells.[44,45] Hydrophobic sites include for example the ribose carbon atoms, H-bond donor sites include the amino ($-NH_2$) groups on the nucleobases, and H-bond acceptor sites include, e.g., the oxygen atoms in the phosphate backbone and in the nucleobase carbonyls (see Figure 1b).

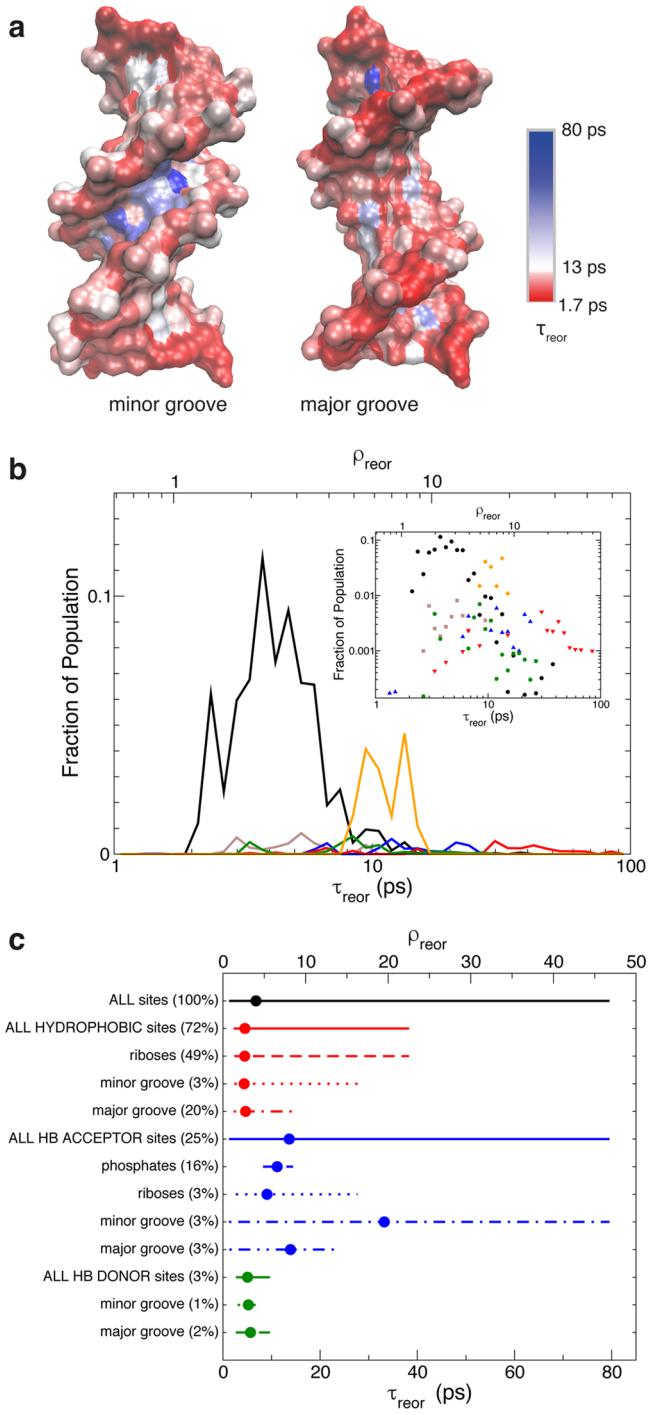

Figure 3. (a) Mapping of the reorientation time τ_{reor} (eq 2) on the DNA surface. (b) Probability distribution of τ_{reor} decomposed by type of DNA site: hydrophobic site (black), H-bond donor (brown), and H-bond acceptors respectively in the major (blue) and minor (red) grooves, on the ribose (green) and phosphate (orange) groups. The same distributions, with the same color code, are shown in the inset on a log−log scale. (c) Water reorientation time and slowdown for each type of DNA site, where each line shows the range of values and the dot gives the average value.

This decomposition is shown in Figure 3b, while Figure 3c further provides—for each type of site (hydrophobic, H-bond donor, H-bond acceptor) and for different locations of such sites (e.g., on DNA bases in the minor groove)—the mean reorientation time and corresponding retardation factor,

DOI: 10.1021/jacs.6b02715
J. Am. Chem. Soc. 2016, 138, 7610−7620

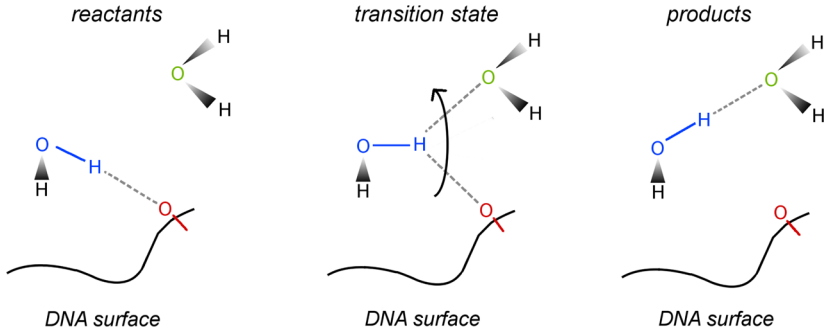

Figure 4. Schematic representation of the jump mechanism, shown for the example of a jump from a DNA H-bond acceptor to a water oxygen H-bond acceptor. Such jumps can also occur from water to DNA, between two DNA acceptor sites, and between two water molecules in the vicinity of DNA.

together with the range of slowdown observed for such sites. This shows that the principal peak, containing approximately 73% of the hydration shell and exhibiting weakly perturbed water dynamics (ρ < 4.5), arises mainly from hydrophobic exposed sites, i.e., from the ribose and nucleobase carbon atoms, with a minor contribution from H-bond donor sites, i.e., $-NH_2$ groups in the nucleobases (see Figure 1b). The intermediate peak at moderate slowdown values (4.5 < ρ < 10, peak absent in proteins[44,45]) contains ∼24% of the hydration shell and corresponds to water reorientation at the phosphate backbone sites. Finally, the small amplitude tail extending to large slowdown values (ρ > 10) originates from ∼10 water molecules which are located in the spine of hydration and which donate a H-bond to a minor-groove site, e.g., to a thymine carbonyl oxygen atom (see Figure 1b). We will show below that such slowdown factors for these different types of sites should be expected from our prior work[42] on the effect of solutes on water dynamics. The reorientation times of these slow water molecules (ranging from ∼20 to ∼80 ps) are consistent with, although somewhat faster than, the ∼0.2 ns correlation time obtained by NMR at ambient temperature.[8] (We pause to note that NMR dispersion experiments probe the single molecule water rotational dynamics and the comparison with our reorientation times is therefore meaningful; this time is usually designated as a residence time in the NMR literature because of the simplified model used to analyze the spectral density and that assumes that water reorientation is caused by either the escape from the DNA hydration shell or the slow DNA tumbling.[8,46]) These times are also in very good agreement with prior reorientation and residence time calculations (see, e.g., refs 10, 32, and 40).

We finally note that the reorientation of these water molecules occurs on a time scale close to the 20 ps time measured by TDSS.[9] We do not find any water molecule reorienting on the extremely slow (>1 ns) time scale observed in some[29,47] TDSS studies. The TDSS signal is sensitive to long-range collective effects and to coupled water-DNA motions, and this debated ns component has been suggested to possibly arise, e.g., from specific DNA dynamics caused by the structural damage induced by the synthetic base[48] or from ion atmosphere rearrangements.[27,49] In contrast, our present simulations show that the dynamics of individual water molecules within the DNA hydration shell do not exhibit such a ns component.

Molecular Origin of Spatial Heterogeneity. We now provide a molecular interpretation of why and how the hydration dynamics is influenced by DNA, and we identify which molecular features induce the great variations visible in Figure 3 in the reorientational slowdown among sites. Our goal is to elucidate the respective importance of the DNA exposed surface topography, of confinement and of the H-bond strength in the perturbation. We will use the extended jump model for water reorientation dynamics,[42,50] which explicitly describes these different effects. Two of us showed that the reorientation dynamics of water are mostly governed by sudden large-amplitude angular jumps occurring when a water OH group switches H-bond acceptors[42,50] (see Figure 4). This molecular jump mechanism was established to apply not only in the bulk but also in the vicinity of a broad range of solutes, including ions,[51] amphiphilic molecules,[52,53] and proteins.[44]

We first confirm that angular jumps—which exchange H-bonding partner for the reorienting water OH bond[50]—remain the main mechanism for water reorientation in DNA hydration shells. To this end, the standard reorientation TCF C_{reor} (eq 1) for all first shell water molecules is compared to C_{reor} restricted to the trajectory time intervals when the water molecules do *not* execute a jump to a new H-bond acceptor (Figure 2). It is seen that now reorientation is much slower without jumps: C_{reor} reaches a plateau value that reflects the limited range of orientations accessible without exchanging H-bonds. This establishes the jumps' critical importance in reorientation. In the absence of H-bond jumps, a water molecule can neither leave the DNA first hydration shell to enter the bulk, nor execute a large-amplitude rotation while staying in the DNA first hydration shell. Further, we need to recognize that water jumps can occur toward either another water molecule or toward a DNA H-bond acceptor. However, Figure 2 shows that jumps toward a water acceptor are much more important for reorientation, since jumps to a DNA site do not allow the water molecule to exit the hydration shell. We conclude that jumps to water molecules are the dominant molecular mechanism responsible for the reorientation dynamics. Therefore, the heterogeneity in hydration shell reorientation dynamics must be caused by a broad underlying distribution in water jump times. This critical conclusion is also confirmed by the great similarity between the distributions of reorientation and jump slowdown factors in the shell (see Figures S2 and S3).

Jump H-bond exchanges can be viewed as chemical reactions where an original H-bond is broken and a new one is formed.[42,50] The jump dynamics are probed by the probability for an OH group initially stably H-bonded to a given acceptor I *not* to have jumped to form a new stable H-bond with any final acceptor F after a given delay. It is defined by

DOI: 10.1021/jacs.6b02715
J. Am. Chem. Soc. 2016, 138, 7610−7620

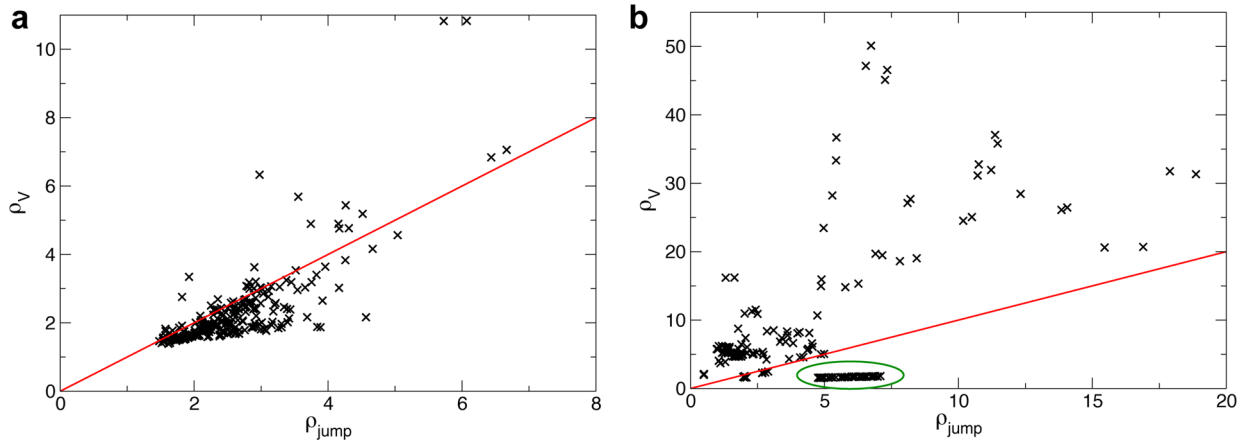

Figure 5. Comparison of the computed TSEV slowdown factor[52] ρ_V at each DNA site compared with the slowdown factor ρ_{jump} directly obtained in our simulations, (a) for DNA hydrophobic and H-bond donor sites and (b) for H-bond acceptor sites. Phosphate acceptor sites are circled in green. In both panels, the red line shows the $\rho_V = \rho_{jump}$ reference. (For acceptors, the excluded volume factor gives a crude prediction of the slowdown factor, because the strength of the initial H-bond should also be considered.)

$$C_j(t) = 1 - \langle n_I(0) n_F(t) \rangle \quad (3)$$

where in this TCF $n_{I,F}(t) = 1$ if the OH bond forms a stable[54] H-bond at time t respectively with the I,F acceptors (as guaranteed by absorbing boundary conditions), and $n_{I,F}(t) = 0$ otherwise.[55] The jump time is then obtained by time-integration of C_j for each DNA site $\tau_j = \int_0^\infty C_j(t)dt$.

The jump free energy transition state barrier results both from the initial H-bond elongation—sensitive to the initial H-bond strength—and from the new partner's approach—affected by the excluded volume induced for example by hydrophobic groups and confinement; these two effects on the jump rate constant have been incorporated in an extended jump model.[50] Prior work employing this model has determined how jump kinetics is affected by the presence of neighboring solutes.[42] A detailed investigation of the extended jump model for DNA hydration dynamics focused on short time dynamics will be presented elsewhere, but we already offer here a brief molecular interpretation of the different slowdown factors in the distribution Figure 3b.

The hydrophobic sites causing the large peak at $\rho < 4.5$ do not form H-bonds with shell water molecules; rather, they retard the jump dynamics by hindering the approach of a new water acceptor. The slowdown induced by these hydrophobic groups is determined within the jump transition state excluded volume (TSEV) model[52] by the fraction of jump transition state configurations for a new water H-bond acceptor that are blocked by the DNA dodecamer. Figure 5a shows how the computed TSEV slowdown factor ρ_V[52] at each site compares with the slowdown factor directly obtained in our simulations $\rho_{jump} = \tau_j/\tau_j^{bulk}$. For hydrophobic and H-bond donor DNA sites, the agreement between the TSEV model and the water reorientation slowdown obtained from our simulations is fairly good. This strongly supports the view that water dynamics at these sites mainly depend on the local topography of the DNA exposed surface. This excluded-volume factor explains why convex sites protruding into the aqueous solution typically lead to $\rho < 2$[52] while concave sites induce a larger slowdown $\rho > 2$[52,56] due to confinement.

For the reorientation of water next to H-bond acceptor groups, the excluded volume alone is not sufficient to account for the slowdown in the dynamics (Figure 5b). An especially important instance of this is the water molecules next to the phosphate backbone sites. Here the slowdown induced in these sites' hydration shell dynamics arises not only from the above-described excluded-volume effect which remains limited (see Figure 5b); it also has an important contribution from the strength of the phosphate−water H-bond, which needs to be activated by elongation to reach the jump transition state. This H-bond is stronger than that between two water molecules (see, e.g., ref 57) and causes an additional slowdown with respect to the bulk,[53] explaining the larger ρ values reported for these exposed sites ($4.5 < \rho < 10$). The long-lived phosphate−water H-bond that we find (with a ≃20 ps H-bond jump time) is consistent with the 10 ps lower bound obtained via time-resolved infrared spectroscopy of phosphate hydration dynamics in aqueous solution[58] and in phospholipid reverse micelles[59] (However, it does not corroborate an NMR study's suggestion of bulk-like dynamics around DNA phosphate groups.[18])

Finally, we found that an initial simple analysis was insufficient to explain the behavior of the 10 very slow ($10 < \rho < 50$) water molecules in the dodecamer minor groove. It is these molecules that cause such a slow component in the hydration shell dynamics (Figure 2) whose existence, time scale and most of all whose origin have been subjects of controversy.[9,30,41] We will consider in detail the behavior of these water molecules in the following; while they represent a very small fraction of the hydration shell, their role in the recognition, binding and intercalation processes may prove to be critical since they lie next to the bases where the genetic information is stored and which cover intercalation sites. As will be seen, both the great confinement within the narrow minor groove and the strong H-bonds with the nucleobases contribute to their slow jump dynamics.

Dynamical Disorder Due to Conformational Fluctuations. We have so far shown that the variety of both local topographies and chemical natures of the DNA exposed sites cause a broad distribution in the hydration shell dynamics. However, this spatial heterogeneity is not the sole source of shell dynamics heterogeneity. This clearly appears for the hydration dynamics next to one given site at a time, without spatial averaging. We elucidate these "single site dynamics" by focusing on the jump dynamics probed by the jump TCF and associated jump time as defined in eq 3.

DOI: 10.1021/jacs.6b02715
J. Am. Chem. Soc. 2016, 138, 7610−7620

For sites well exposed to solvent, $C_j(t)$ follows a single exponential decay, shown for one such site (labeled η) in Figure 6a. Thus, a single jump rate constant k_j governs the dynamics and $C_j(t) = \exp(-k_j t)$. We then choose another site, labeled Σ, now representative of H-bond acceptor sites in the center of the minor groove, in the region rich in adenine·thymine purine base pairs (see Methods). For this acceptor, in contrast to the solvent-exposed site η, C_j exhibits a strongly nonexponential decay (Figure 6a). We stress that this nonexponential behavior is not due to spatial averaging (in contrast with the result in Figure 2 and, e.g., in ref 32, see the Supporting Information), because here we consider each site individually. Evidently at this site an attempted jump rate constant definition is not invariant with time in the trajectory, and—in the strongly nonexponential case—a "rate constant" no longer has an unambiguous meaning: any assigned value would depend on the time interval considered. By contrast with the spatial heterogeneity described above, we will call this additional heterogeneity source a *temporal heterogeneity*, or alternately—as we will see—a dynamical disorder in Zwanzig's stochastic analysis language.[43]

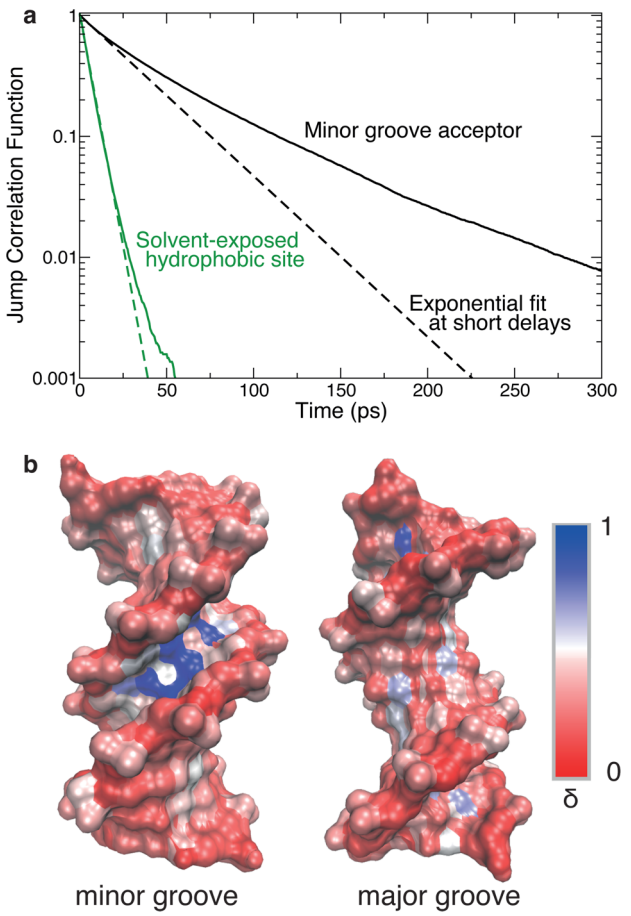

Figure 6. (a) Site-resolved jump TCF (eq 3) (solid lines) for water molecules initially H-bonded to one of the two acceptor sites Σ at the center of the A-tract, in the minor groove (black) and for a solvent-exposed hydrophobic site η (green), together with exponential fits (dashes) on the 0–5 ps interval (see Methods for site definitions). (b) Mapping of the temporal heterogeneity δ (eq 4) on the DNA surface.

At each DNA site, the degree of temporal heterogeneity can be conveniently determined by analyzing the observed jump events via the distribution of H-bond lifetimes τ_{HB}. We define here the (unconventional) lifetime as the time interval between formation of a stable H-bond with its initial acceptor, and formation of a new stable H-bond with a different acceptor (see the Supporting Information). This definition thus properly ignores transient breaks and has the further advantage of being fairly insensitive to the precise definition of the H-bond. At a site with a single k_j value, the statistics is Poissonian and the τ_{HB} distribution is exponential, $p(\tau_{HB}) = k_j \exp(-k_j\tau_{HB})$. In contrast, at sites with a range of k_j values (see below), this heterogeneity induces a departure from the exponential reference quantifiable via the τ_{HB} distribution's first and second moments through the temporal heterogeneity parameter δ[60]

$$\delta = \frac{\langle \tau_{HB}^{\,2} \rangle}{2\langle \tau_{HB} \rangle^2} - 1 \tag{4}$$

Figure 6b presents the map of δ at every DNA site (with $\delta = 0$ by construction if no heterogeneity is present). It clearly shows that while the temporal heterogeneity is very limited next to solvent-exposed sites (e.g., the phosphate backbone), it is more pronounced for a number of sites located in both grooves. A moderate temporal heterogeneity is found in the major groove (δ up to 0.55), while the strongest temporal heterogeneity—and thus the largest deviation from an exponential decay of the jump TCF—is found in the central part of the minor groove ($\delta > 0.7$), precisely where water dynamics are markedly slow.

In order to determine the molecular factors that cause this heterogeneity, we now focus on the central minor-groove site Σ in the A·T-rich region where δ is very large. We will contrast dynamics for this site with those for the site designated σ on the end of the minor groove, where the temporal heterogeneity is very limited. (see Methods for site definitions). As will be shown below, the ideas now developed also apply to the major groove sites, although the temporal heterogeneity found there is less pronounced.

We showed above that the water jump dynamics are sensitive to the DNA exposed surface's local topography. However, the DNA interface's shape is not fixed: it fluctuates with the DNA conformational motions. The impact of these changes is especially strong in the minor groove, where they affect the degree of confinement and therefore the induced slowdown of the water molecules. Figure 7a shows that for waters in the Σ central minor-groove site, $C_j(t)$ is very sensitive to the initial minor groove width (Several groove width definitions exist; we adopt one that probes the motions relevant for the water dynamics (see Figure S5)).

It is important to stress the molecular origin of this modulation of the jump dynamics by the groove width. The jump model established that the approach of a new H-bond partner is a key part of the rate-limiting step.[52] Consequently, the more narrow is the DNA groove, the slower are the jump dynamics because the approach of a new H-bond partner is increasingly hindered. The DNA movements thus do not directly "push" the water molecule that reorients; instead the slow water dynamics results from narrow groove geometries. This is markedly different from an interpretation that has been suggested[61] for TDSS experiments on protein hydration dynamics. There the very slow changes in the water contribution to the electronic transition energy were explained by water molecules being displaced by very slow biomolecular motions, so that the slow TDSS time scale would be the biomolecular relaxation time. The situation here is in strong contrast to this: suppression of the slow DNA motions by

DOI: 10.1021/jacs.6b02715
J. Am. Chem. Soc. 2016, 138, 7610–7620

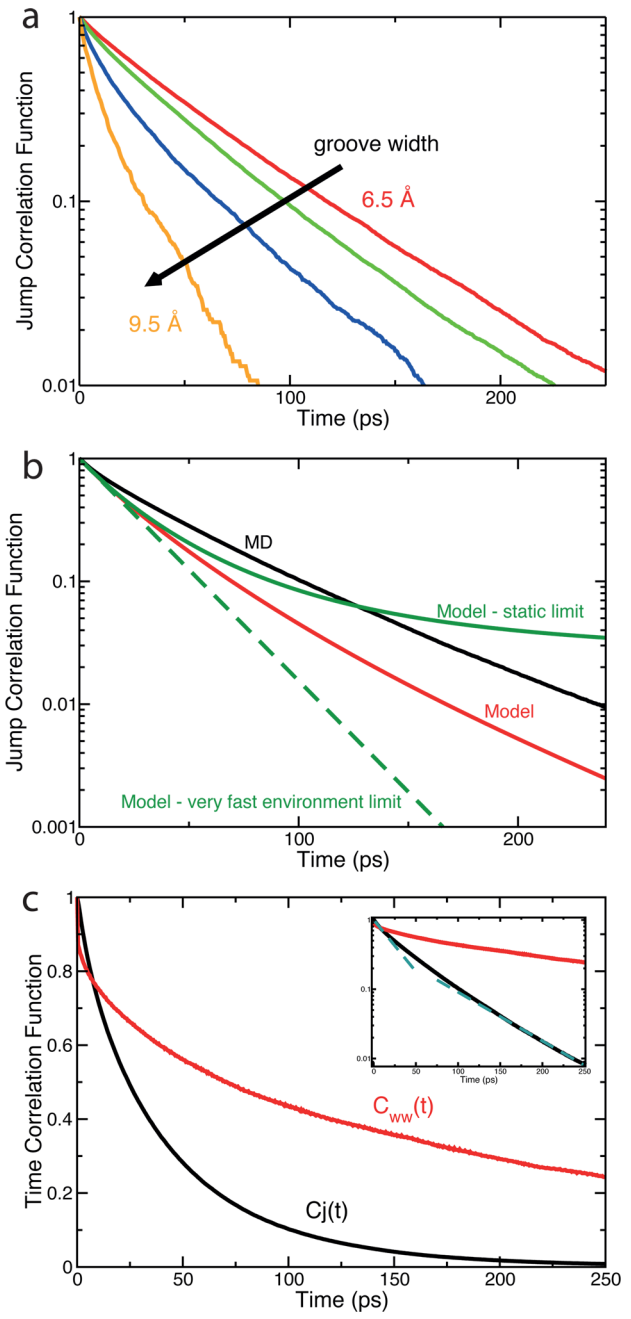

Figure 7. (a) Jump TCF (eq 3) for water molecules in a bridging configuration at the central acceptor site Σ of the DNA sequence, for different initial minor groove widths. (b) Jump TCF C_j computed respectively directly from the MD simulations (eq 3) (black) and from the dynamical heterogeneity model (eq 5) (red), together with the very fast (green dashes) and very slow (solid green) environment dynamics limits. (c) Minor groove width TCF $C_{ww}(t)$ (eq 6) (red) and jump TCF (eq 3) (black) at the central minor groove site Σ together with a semilog representation in inset including short- and long-time exponential fits of C_j (green dashes).

freezing the DNA conformation retards the jump dynamics even more than when DNA is flexible (see Figure S13).

We pause to note that water molecules can adopt two different H-bond arrangements in the narrow DNA minor grooves. Waters can be either in a "bridging" configuration where they donate two H-bonds to DNA sites (one per hydrogen atom), or in a "nonbridging" configuration where they donate one H-bond to DNA and another to a water molecule.[33−35] These two arrangements exhibit different dynamical behaviors; we focus here on the "bridge" population which dominates the overall A·T-rich region dynamics (see Figure S6).

The DNA conformational motions can therefore affect the jump rate behavior. We now present a simple stochastic model that connects the DNA groove width fluctuations to the nonexponential character of the water jump TCF and thus to the temporal heterogeneity in the hydration dynamics, i.e., to the dynamical disorder.[43] We stress that the goal of this model is not to yield a quantitative description of the heterogeneity; it is instead to identify the key molecular factors explaining why the temporal heterogeneity, i.e., the C_j nonexponential behavior, varies dramatically over the different DNA sites.

We first determine a jump rate constant k_j for different initial groove width values w. For the stochastic model, we will define this by the initial slope of the $\ln[C_j(t)^{(w)}]$ decay for a given initial w. We then approximate the groove-width dependence of this k_j with a linear fit $k_j(w) = \alpha + \beta w$ (see Figure S9). Since w can vary with time, this rate constant now becomes a parametric function of time. The jump TCF (eq 3) is a survival probability which in our model we assume can be numerically computed from the groove width time evolution only,[62]

$$C_j(t) = \langle \exp(-\int_0^t k_j[w(t')]\mathrm{d}t') \rangle \tag{5}$$

Figure 7b shows that our simple model (eq 5) predicts a strongly nonexponential $C_j(t)$ and succeeds in capturing a large fraction of the impact of the heterogeneity in the jump TCF (eq 3) computed directly from the MD simulation. This confirms that the site rate modulation by groove fluctuations plays an essential role in the jump temporal heterogeneity measured in the minor groove center and in the magnitude of the average slowdown.

The degree of temporal heterogeneity in each DNA site could fall between two possible limiting cases. The first limit would arise if the relevant DNA structural dynamics at the site were so slow that each jump occurred in a fixed, possibly different environment, i.e., minor groove width. With a distribution of widths at site j, the average C_j (eq 5) would be an average of exponential decays $\exp(-k_j t)$ over the static distribution of different groove width structures, each structure associated with its own k_j, i.e., $C_j(t) \simeq \langle \exp(-k_j t) \rangle$. This is similar to the slow modulation (inhomogeneous) limit in Kubo's spectral lineshape theory,[63,64] where the heterogeneity is maximal. The other extreme would be reached if the DNA structural dynamics were so fast that the full groove width distribution was sampled before the jump occurred, and jumps took place with an average rate constant, thus suppressing any observable heterogeneity in the dynamics for the site, leading to the different exponential decay $C_j(t) \simeq \exp(-\langle k_j \rangle t)$. This situation is analogous to the equilibrium solvation picture for chemical reactions[65] and to the fast modulation (homogeneous) limit in spectroscopy,[63,64] where motional narrowing hides the underlying heterogeneity.

Figure 7b shows that, in the A·T minor groove, the directly simulated C_j decay lies between the very slow extremely nonexponential static limit and the fast homogeneous decay, both numerically determined with our model (eq 5). Therefore, neither limiting situation applies. The reason for this is that there is no real time scale separation, i.e., the time scales for the

DOI: 10.1021/jacs.6b02715
J. Am. Chem. Soc. 2016, 138, 7610−7620

groove width fluctuations and the H-bond jump are similar. This similarity is evident in Figure 7c which shows a comparison of the jump (eq 3) and groove width TCF

$$C_{ww}(t) = \frac{\langle \delta w(0)\delta w(t)\rangle}{\langle \delta w^2\rangle} \quad (6)$$

where $\delta w(t) = w(t) - \langle w\rangle$ is the instantaneous fluctuation of the minor groove width $w(t)$ with respect to its average $\langle w\rangle$. This similarity underlines the importance of the DNA conformational dynamics in the extent of this dynamical disorder. We note that we have obtained similar results for major groove sites. Although the major and minor groove fluctuations are uncorrelated (see the Supporting Information), the jump rate is found to vary with the major groove width and the groove width fluctuates on a time scale similar to that of the jumps. However, the resulting heterogeneity is more moderate than in the minor groove for two reasons: the major groove is typically broader than the minor groove and the approach of a new H-bond partner is not as strongly dependent on the groove widening (see Figure S12).

Our results also show that the static picture limit—which is widely used to describe biomolecular hydration dynamics and interpret experimental data[8,46,66,67]—is not valid here, because that limit incorrectly assumes that the water dynamics is much faster than the biomolecular conformational motions. This is further supported by a series of direct simulations on frozen DNA conformations, where the water dynamics are found to be much slower than the average dynamics with a flexible DNA (see Figure S13). These results unambiguously show that the slow hydration dynamics do not arise from coupled water−DNA motions. In addition, they demonstrate that minor groove hydration dynamics cannot be modeled by exchanges between two states—a wide-groove conformation where water dynamics are fast and a narrow-groove state where water dynamics are extremely slow[15]—since this would lead to a biexponential decay of C_j whose slow time scale would be the groove width fluctuation time. In contrast, Figure 7c shows that even in narrow grooves, water dynamics are not much slower than the groove conformational dynamics and the C_j decay is not biexponential (inset, Figure 7c).

We can further use this simple model to identify the molecular factors that—even though DNA conformational motions occur all along the sequence—cause the minor groove heterogeneity to be much larger in the sequence center than at the ends of the strand (Figure 6b). To this end, and for the sole purpose of obtaining qualitative insights into this issue, we make the rather crude second-order cumulant expansion approximation (see, e.g., ref 64) for the stochastic survival probability formulation of the jump TCF (eq 5), leading to[62]

$$C_j(t) \simeq \exp[-\langle k_j\rangle t + \langle \delta k_j^2\rangle \int_0^t (t - t')C_{kk}(t')\mathrm{d}t'] \quad (7)$$

where $\langle k_j\rangle$ is the static average of k_j over the minor groove width distribution and $C_{kk}(t)$ is the TCF of the $k_j(t)$ fluctuations around this average, $C_{kk}(t) = \langle \delta k_j(0)\delta k_j(t)\rangle/\langle \delta k_j^2\rangle$.

The comparison of the C_j decay rates in this representation at short and long time delays provides an intuitive probe of the departure from simple exponential decay and important aspects of the degree of temporal heterogeneity. At very short delays, its exponential relaxation rate is[62] $k_{short} = \langle k_j\rangle$; importantly, this gives also the $C_j(t)$ result for rapid width dynamics, and we will use $\langle k_j\rangle$ as our reference for the jump rate. At delays much longer than τ_k the decay slows and becomes[62] $k_{long} = \langle k_j\rangle$ [1−($\langle \delta k_j^2\rangle/\langle k_j\rangle$) τ_k], where $\langle \delta k^2\rangle$ and $\tau_k = \int_0^\infty C_{kk}(t)\mathrm{d}t$ respectively provide the key measures of the amplitude and relaxation time scale of the width fluctuations.

The disparity between k_{short} and k_{long} described by

$$1 - \frac{k_{long}}{k_{short}} = \frac{\langle \delta k_j^2\rangle}{\langle k_j\rangle}\tau_k = \frac{\langle \delta k_j^2\rangle}{\langle k_j\rangle^2}\langle k_j\rangle\tau_k \quad (8)$$

thus measures the nonexponential character of C_j. It is the product of two terms: the first, $\langle \delta k_j^2\rangle/\langle k_j\rangle^2$, depends on the (static) rate constant distribution's relative width, and the second, $\langle k_j\rangle\tau_k$, assesses the dynamical aspects via the jump and structural fluctuation time scales. Dynamical disorder arises from the combination of three concomitant factors: (i) the presence of a broad distribution of k_j rate constants, which is sampled by (ii) conformational motions not fast enough to sample the full distribution before (iii) the fast H-bond jump occurs.

We now compare the values of each of these terms in eq 8 for the central site Σ where the heterogeneity is strong (δ = 1.2) and for site σ at the minor groove end where the heterogeneity is much smaller (δ = 0.29). These numbers should be considered only qualitatively since they involve an approximate linear relationship between the model k_j and w, and require decomposing the water molecules into bridging and nonbridging configurations (respectively donating two or one H-bonds to DNA, as described above). We find that the dynamical term $\langle k_j\rangle\tau_k$ varies little between the two sites (6.6 in Σ vs 9.3 in σ) since the DNA conformational fluctuations at the two sites induce similar jump rate fluctuation time scales ($\tau_k^\Sigma \simeq$ 190 ps vs $\tau_k^\sigma \simeq$ 180 ps) and the jump rate constant is moderately larger at the sequence's end ($\langle k_j^\Sigma\rangle \simeq$ 35 ns^{-1} vs $\langle k_j^\sigma\rangle \simeq$ 52 ns^{-1}). In contrast, the static fluctuation term $\langle \delta k_j^2\rangle/\langle k_j\rangle^2$ exhibits a much larger variation (approximately 0.34 in Σ vs 0.03 in σ); this variation is due not to different amplitudes of groove width fluctuations in the two sites, but rather to the different sensitivities of k_j to w, i.e. different β slope values. A slight groove widening in the central Σ site has a much larger impact on k_j than the same broadening in the σ site where the groove is already broader.

These results show that the temporal heterogeneity change along the DNA base pair sequence is most likely due to variation in the rate constant distribution's width. We stress, to avoid potential confusion, that the heterogeneity itself is of dynamical origin, as we have shown, but its *variation* along the minor groove is evidently due to a change in the static distribution of jump rates rather than a change in the groove dynamics.

A final comment is due concerning the potential implication of the Na^+ ions in the hydration dynamical heterogeneity we have reported, since sodium ions can penetrate in the DNA first hydration shell and replace water molecules in the minor groove.[36,68] Our results obtained with minimum salt conditions show that while groove-bound water molecules exhibit faster dynamics when in contact with an ion, such penetration is a very exceptional event; in agreement with prior works[40,69] (see the Supporting Information), an ion is found at the minor groove site σ in less than 2% of our simulation time (see Figure S11). In addition and more importantly, the groove temporal heterogeneity is found to persist in the absence of any ion in the vicinity; this confirms that this dynamical disorder is not due to the ion atmosphere.

DOI: 10.1021/jacs.6b02715
J. Am. Chem. Soc. 2016, 138, 7610−7620

CONCLUDING REMARKS

The hydration layer of DNA is essential for its conformation and its function. Its lability and dynamics can for example significantly affect the binding of proteins and ligands, and the intercalation of anticancer drugs. However, some key aspects of this layer's dynamical properties have remained very unclear, including the presence of some very slow water molecules, and if present, the cause of their slowness. We have presented here a detailed analysis of, and provided important new insights into, water dynamics in the DNA hydration shell, all informed by the jump picture for these dynamics. We revealed the presence of different sources of heterogeneity in the hydration shell dynamics. We first showed that the hydration dynamics change dramatically in the different DNA exposed sites, leading to a strong spatial heterogeneity. The jump model was used to distinguish the effects of the DNA interfacial topography and of the DNA−water H-bond interactions. While most of the hydration shell is only moderately retarded with respect to bulk water by hydrophobic groups and by attraction to phosphate groups, a small number of very slow water molecules with reorientation times between 30 and 85 ps (slowdown factor 20−50) were found in the minor groove's central adenine·thymine-rich region.

Furthermore, we revealed here a new, additional source of heterogeneity, which is especially strong for water molecules in the spine of hydration running along the narrow DNA minor groove. This additional, temporal heterogeneity is caused by groove conformational fluctuations, which modulate the water jump dynamics and lead to a broad distribution of water reorientation times at a given DNA site in the minor groove. While the presence of water affects the DNA conformation and dynamics, our results showed that the minor groove water dynamics are modulated by the slow DNA motions, because the groove widening facilitates the approach of a new water partner and accelerates the H-bond jump. This is in stark contrast with suggestions that the dynamics of biomolecules are slaved to their hydration shell,[70] and our results demonstrate that the widely used static limit which assumes that water dynamics are much faster than biomolecular conformational motions is not valid in the DNA minor groove and probably in other confined biomolecular hydration sites.

Future work will extend the present study to DNA in aqueous solutions with physiological ionic concentrations. We anticipate that the impact of cations on the hydration shell dynamic disorder will depend on both their residence time[68,71,72] and effect on the groove width[36,73] (see Figure S11). Finally, the detailed molecular understanding of DNA hydration dynamics gained in the present work will be extremely valuable in the study of how the slow water dynamics can potentially induce a friction on the motion of a ligand or a drug molecule and affect the binding and intercalation kinetics.

METHODS

Molecular Dynamics Simulations. Two independent 200 ns classical molecular dynamics simulations of the B-DNA dodecamer[34] are performed in the NVE ensemble with the AMBER99-parmbsc0[69,74] force field in a box of water molecules, with minimum salt conditions. The parmbsc0 force-field corrections[69] were shown to provide a good description of the minor groove spine of hydration.[75] The dodecamer is solvated in a box of 8756 water molecules described by the SPC/E model, which correctly reproduces water dynamics at room temperature.[55] We use minimum salt conditions with 22 Na^+ ions to neutralize the phosphate charges. The trajectory is propagated with NAMD[76] using a 1 fs time step. Periodic boundary conditions are applied, and long-range electrostatic interactions are treated with the particle mesh Ewald method. Nonbonded interactions are brought smoothly to zero using a switching function from 10 Å to the cutoff of 12 Å. Bonds between hydrogen and heavy atoms are constrained using the SHAKE and SETTLE algorithms.

Hydration Shell Definition. The hydration shell definition and the spatially resolved analysis of hydration shell dynamics follow the same methodology as that used for protein hydration shells in previous work.[44,45] The hydration shell is defined to include all the water OH groups that are H-bonded to or within hydrophobic cutoff of the dodecamer surface, as now explained. Each water OH group within the shell is then assigned to a DNA surface site using the following procedure. The dodecamer surface is divided into H-bond acceptor, H-bond donor and hydrophobic sites. Hydrophobic radii and H-bond geometric criteria are determined for each site from the first minimum of the radial distribution functions between the water oxygen atom and the relevant DNA atom. Typical resulting criteria are $R_{co} < 4.5$ Å for a hydrophobic site, and $R_{da} < 3.5$ Å, $R_{ah} < 2.5$ Å, and $\theta_{hda} < 30°$, for a H-bond, where c is a DNA carbon atom, o is a water oxygen atom, a is a H-bond acceptor atom, d a H-bond donor atom, and h a DNA or water hydrogen atom. Where the assignment of an OH group is ambiguous, sites are given the priority acceptor > donor > hydrophobe, as this has been shown in the protein case to be the order of greatest influence on water reorientational dynamics.[44] This procedure is used to assign water OH bonds to a given DNA site at the TCF time origin. Our study focuses on the first hydration shell, because the dynamical perturbation induced by the DNA falls off rapidly with distance from the surface (Figure S1). The analysis of water and H-bond jump dynamics follow prior work.[45,55] Further details are given in the Supporting Information.

Definitions of DNA Sites Selected for Heterogeneity Analysis. Our analysis of the temporal heterogeneity δ in the AATT region is illustrated for 3 typical sites: a minor groove acceptor site Σ where δ is large ($\delta = 1.2$), a minor groove acceptor site σ where δ is smaller ($\delta = 0.29$), and a hydrophobic site η, that is well exposed to the solvent ($\delta = 0.04$). Σ is the H-bond acceptor O2 oxygen atom of the thymine base occupying the 7^{th} position in the dodecamer sequence, in the narrow minor groove AATT region, which can be viewed as a short A-tract (see Figures 1 and S4). Because of the symmetry of the dodecamer sequence, site Σ is equivalent to the thymine 19 site Σ′ on the opposite strand. The choice of Σ is motivated both by the high temporal heterogeneity δ found at this site and by the symmetry of the Σ and Σ′ sites which simplifies the kinetic analysis of water dynamics. The low δ, minor-groove acceptor site σ is the N3 atom of the guanine base occupying the fourth position in the dodecamer sequence. The hydrophobic site η is the ribose C3′ atom belonging to the fourth nucleotide in the dodecamer.

ASSOCIATED CONTENT

Supporting Information

The Supporting Information is available free of charge on the ACS Publications website at DOI: 10.1021/jacs.6b02715.

Details of the H-bond jump analysis, definition of the minor-groove width, analysis of minor-groove bridge configurations and impact of ions. (PDF)

AUTHOR INFORMATION

Corresponding Authors

*james.hynes@spot.colorado.edu

*damien.laage@ens.fr

Present Address

⊥A.C.F.: Max Planck Institute for Polymer Research, Ackermannweg 10, 55128 Mainz, Germany.

Author Contributions

‖E.D.-D. and A.C.F. contributed equally to this work.

DOI: 10.1021/jacs.6b02715
J. Am. Chem. Soc. 2016, 138, 7610−7620

Notes

The authors declare no competing financial interest.

■ ACKNOWLEDGMENTS

The authors gratefully thank Thomas Elsaesser (Max Born Institut, Berlin) for stimulating discussions and Fabio Sterpone (now at IBPC, Paris) and Philipp Marquetand (now at IPC, Jena) for early work on short time aspects of this problem. This work was supported by Agence Nationale de la Recherche (Grant ANR-2001-BSV5-027-02 to D.L.) and by NSF (Grant CHE-1112564 to J.T.H.), and was performed using HPC resources from GENCI-TGCC (Grant 2014-077156).

■ REFERENCES

(1) Saenger, W.; Hunter, W. N.; Kennard, O. *Nature* **1986**, *324*, 385−388.
(2) Middleton, C. T.; de La Harpe, K.; Su, C.; Law, Y. K.; Crespo-Hernández, C. E.; Kohler, B. *Annu. Rev. Phys. Chem.* **2009**, *60*, 217−239.
(3) Pal, S. K.; Zewail, A. H. *Chem. Rev.* **2004**, *104*, 2099−2124.
(4) Nguyen, B.; Neidle, S.; Wilson, W. D. *Acc. Chem. Res.* **2009**, *42*, 11−21.
(5) Jayaram, B.; Jain, T. *Annu. Rev. Biophys. Biomol. Struct.* **2004**, *33*, 343−61.
(6) Wilhelm, M.; Mukherjee, A.; Bouvier, B.; Zakrzewska, K.; Hynes, J. T.; Lavery, R. *J. Am. Chem. Soc.* **2012**, *134*, 8588−8596.
(7) Mukherjee, A.; Lavery, R.; Bagchi, B.; Hynes, J. T. *J. Am. Chem. Soc.* **2008**, *130*, 9747−9755.
(8) Denisov, V. P.; Carlström, G.; Venu, K.; Halle, B. *J. Mol. Biol.* **1997**, *268*, 118−136.
(9) Pal, S. K.; Zhao, L.; Zewail, A. H. *Proc. Natl. Acad. Sci. U. S. A.* **2003**, *100*, 8113−8118.
(10) Pal, S.; Maiti, P. K.; Bagchi, B. *J. Chem. Phys.* **2006**, *125*, 234903.
(11) Liepinsh, E.; Otting, G.; Wüthrich, K. *Nucleic Acids Res.* **1992**, *20*, 6549−6553.
(12) Pal, S. K.; Zhao, L.; Xia, T.; Zewail, A. H. *Proc. Natl. Acad. Sci. U. S. A.* **2003**, *100*, 13746−13751.
(13) Andreatta, D.; Pérez Lustres, J. L.; Kovalenko, S. A.; Ernsting, N. P.; Murphy, C. J.; Coleman, R. S.; Berg, M. A. *J. Am. Chem. Soc.* **2005**, *127*, 7270−7271.
(14) Zhou, D.; Bryant, R. G. *J. Biomol. NMR* **1996**, *8*, 77−86.
(15) Johannesson, H.; Halle, B. *J. Am. Chem. Soc.* **1998**, *120*, 6859−6870.
(16) Halle, B.; Denisov, V. P. *Biopolymers* **1998**, *48*, 210−233.
(17) Phan, A. T.; Leroy, J.-L.; Guéron, M. *J. Mol. Biol.* **1999**, *286*, 505−519.
(18) Franck, J. M.; Ding, Y.; Stone, K.; Qin, P. Z.; Han, S. *J. Am. Chem. Soc.* **2015**, *137*, 12013−12023.
(19) Szyc, L.; Yang, M.; Nibbering, E. T. J.; Elsaesser, T. *Angew. Chem., Int. Ed.* **2010**, *49*, 3598−3610.
(20) Yang, M.; Szyc, L.; Elsaesser, T. *J. Photochem. Photobiol., A* **2012**, *234*, 49−56.
(21) Polley, D.; Patra, A.; Mitra, R. K. *Chem. Phys. Lett.* **2013**, *586*, 143−147.
(22) Chuprina, V. P.; Heinemann, U.; Nurislamov, A. A.; Zielenkiewicz, P.; Dickerson, R. E.; Saenger, W. *Proc. Natl. Acad. Sci. U. S. A.* **1991**, *88*, 593−597.
(23) Young, M. A.; Ravishanker, G.; Beveridge, D. L. *Biophys. J.* **1997**, *73*, 2313−2336.
(24) Duan, Y.; Wilkosz, P.; Crowley, M.; Rosenberg, J. M. *J. Mol. Biol.* **1997**, *272*, 553−572.
(25) Bonvin, A. M.; Sunnerhagen, M.; Otting, G.; van Gunsteren, W. F. *J. Mol. Biol.* **1998**, *282*, 859−873.
(26) Cheatham, T. E., III; Kollman, P. A. *Annu. Rev. Phys. Chem.* **2000**, *51*, 435−471.
(27) Pal, S.; Maiti, P. K.; Bagchi, B.; Hynes, J. T. *J. Phys. Chem. B* **2006**, *110*, 26396−26402.
(28) Furse, K. E.; Corcelli, S. A. *J. Am. Chem. Soc.* **2008**, *130*, 13103−13109.
(29) Sen, S.; Andreatta, D.; Ponomarev, S. Y.; Beveridge, D. L.; Berg, M. A. *J. Am. Chem. Soc.* **2009**, *131*, 1724−1735.
(30) Furse, K. E.; Corcelli, S. A. *J. Phys. Chem. Lett.* **2010**, *1*, 1813−1820.
(31) Yonetani, Y.; Kono, H. *Biophys. Chem.* **2012**, *160*, 54−61.
(32) Saha, D.; Supekar, S.; Mukherjee, A. *J. Phys. Chem. B* **2015**, *119*, 11371−11381.
(33) Yonetani, Y.; Kono, H. *Biophys. J.* **2009**, *97*, 1138−1147.
(34) Drew, H. R.; Dickerson, R. E. *J. Mol. Biol.* **1981**, *151*, 535−556.
(35) Tsukamoto, T.; Ishikawa, Y.; Natsume, T.; Dedachi, K.; Kurita, N. *Chem. Phys. Lett.* **2007**, *441*, 136−142.
(36) Shui, X.; McFail-Isom, L.; Hu, G. G.; Williams, L. D. *Biochemistry* **1998**, *37*, 8341−8355.
(37) Setny, P.; Baron, R.; Kekenes-Huskey, M. P.; McCammon, J. A.; Dzubiella, J. *Proc. Natl. Acad. Sci. U. S. A.* **2013**, *110*, 1197−1202.
(38) Bastos, M.; Castro, V.; Mrevlishvili, G.; Teixeira, J. *Biophys. J.* **2004**, *86*, 3822−3827.
(39) Nakagawa, H.; Yonetani, Y.; Nakajima, K.; Ohira-Kawamura, S.; Kikuchi, T.; Inamura, Y.; Kataoka, M.; Kono, H. *Phys. Rev. E* **2014**, *90*, 022723.
(40) Furse, K. E.; Corcelli, S. A. *J. Phys. Chem. B* **2010**, *114*, 9934−9945.
(41) Zhong, D.; Pal, S. K.; Zewail, A. H. *Chem. Phys. Lett.* **2011**, *503*, 1−11.
(42) Laage, D.; Stirnemann, G.; Sterpone, F.; Rey, R.; Hynes, J. T. *Annu. Rev. Phys. Chem.* **2011**, *62*, 395−416.
(43) Zwanzig, R. *Acc. Chem. Res.* **1990**, *23*, 148−152.
(44) Sterpone, F.; Stirnemann, G.; Laage, D. *J. Am. Chem. Soc.* **2012**, *134*, 4116−4119.
(45) Fogarty, A. C.; Laage, D. *J. Phys. Chem. B* **2014**, *118*, 7715−7729.
(46) Halle, B. *Philos. Trans. R. Soc., B* **2004**, *359*, 1207−23. discussion 1223−1224, 1323−1328.
(47) Banerjee, D.; Pal, S. K. *J. Phys. Chem. B* **2008**, *112*, 1016−1021.
(48) Furse, K. E.; Corcelli, S. A. *J. Am. Chem. Soc.* **2011**, *133*, 720−723.
(49) Bagchi, B. *Mol. Phys.* **2014**, *112*, 1418−1426.
(50) Laage, D.; Hynes, J. T. *Science* **2006**, *311*, 832−835.
(51) Laage, D.; Hynes, J. T. *Proc. Natl. Acad. Sci. U. S. A.* **2007**, *104*, 11167−11172.
(52) Laage, D.; Stirnemann, G.; Hynes, J. T. *J. Phys. Chem. B* **2009**, *113*, 2428−2435.
(53) Sterpone, F.; Stirnemann, G.; Hynes, J. T.; Laage, D. *J. Phys. Chem. B* **2010**, *114*, 2083−2089.
(54) Northrup, S. H.; Hynes, J. T. *J. Chem. Phys.* **1980**, *73*, 2700−2714.
(55) Laage, D.; Hynes, J. T. *J. Phys. Chem. B* **2008**, *112*, 14230−14242.
(56) Fogarty, A. C.; Coudert, F. X.; Boutin, A.; Laage, D. *ChemPhysChem* **2014**, *15*, 521−529.
(57) Gruenbaum, S. M.; Skinner, J. L. *J. Chem. Phys.* **2011**, *135*, 075101.
(58) Costard, R.; Tyborski, T.; Fingerhut, B. P.; Elsaesser, T. *J. Chem. Phys.* **2015**, *142*, 212406.
(59) Costard, R.; Heisler, I. A.; Elsaesser, T. *J. Phys. Chem. Lett.* **2014**, *5*, 506−511.
(60) Qvist, J.; Schober, H.; Halle, B. *J. Chem. Phys.* **2011**, *134*, 144508.
(61) Nilsson, L.; Halle, B. *Proc. Natl. Acad. Sci. U. S. A.* **2005**, *102*, 13867−13872.
(62) Stirnemann, G.; Laage, D. *J. Chem. Phys.* **2012**, *137*, 031101.
(63) Kubo, R. *Adv. Chem. Phys.* **1969**, *15*, 105−127.
(64) Hamm, P.; Zanni, M. *Concepts and methods of 2D infrared spectroscopy*; Cambridge University Press: Cambridge, UK, 2011.
(65) Gertner, B. J.; Bergsma, J. P.; Wilson, K. R.; Lee, S.; Hynes, J. T. *J. Chem. Phys.* **1987**, *86*, 1377−1386.

DOI: 10.1021/jacs.6b02715
J. Am. Chem. Soc. 2016, 138, 7610−7620

(66) Bryant, R. G. *Annu. Rev. Biophys. Biomol. Struct.* **1996**, *25*, 29−53.
(67) Mattea, C.; Qvist, J.; Halle, B. *Biophys. J.* **2008**, *95*, 2951−2963.
(68) Rueda, M.; Cubero, E.; Laughton, C. A.; Orozco, M. *Biophys. J.* **2004**, *87*, 800−811.
(69) Pérez, A.; Marchán, I.; Svozil, D.; Sponer, J.; Cheatham, T. E.; Laughton, C. A.; Orozco, M. *Biophys. J.* **2007**, *92*, 3817−3829.
(70) Fenimore, P. W.; Frauenfelder, H.; McMahon, B. H.; Parak, F. G. *Proc. Natl. Acad. Sci. U. S. A.* **2002**, *99*, 16047−16051.
(71) Denisov, V. P.; Halle, B. *Proc. Natl. Acad. Sci. U. S. A.* **2000**, *97*, 629−633.
(72) Dans, P. D.; Faustino, I.; Battistini, F.; Zakrzewska, K.; Lavery, R.; Orozco, M. *Nucleic Acids Res.* **2014**, *42*, 11304−20.
(73) Lavery, R.; Maddocks, J. H.; Pasi, M.; Zakrzewska, K. *Nucleic Acids Res.* **2014**, *42*, 8138−8149.
(74) Wang, J.; Cieplak, P.; Kollman, P. A. *J. Comput. Chem.* **2000**, *21*, 1049−1074.
(75) Zhu, X.; Schatz, G. C. *J. Phys. Chem. B* **2012**, *116*, 13672−13681.
(76) Phillips, J. C.; Braun, R.; Wang, W.; Gumbart, J.; Tajkhorshid, E.; Villa, E.; Chipot, C.; Skeel, R. D.; Kale, L.; Schulten, K. *J. Comput. Chem.* **2005**, *26*, 1781−1802.

DOI: 10.1021/jacs.6b02715
J. Am. Chem. Soc. 2016, 138, 7610−7620